Available online at www.sciencedirect.com
ScienceDirect
Journal of the European Ceramic Society 27 (2007) 4711–4717
www.elsevier.com/locate/jeurceramsoc

Fabrication, optical transmittance, and hardness of IR-transparent ceramics made from nanophase yttria

Hergen Eilers *

Institute for Shock Physics, Applied Sciences Laboratory, Washington State University-Spokane, P.O. Box 1495, Spokane, WA 99210-1495, United States

Received 11 February 2007; received in revised form 9 April 2007; accepted 17 April 2007
Available online 7 June 2007

Abstract

Commercially available nanophase yttria powder was used to fabricate a transparent ceramic and its optical transmittance and hardness were measured. The nanophase yttria powder was dry-pressed without the use of any binders. Subsequently, the green body was sintered in air, hot-isostatically pressed, and polished, resulting in an IR-transparent ceramic. Scanning electron microscopy revealed a grain size of 21.5 ± 11.1 μm. Optical transmittance reached about 60% at 1 μm, and hardness measurements showed 792 $HK_{100\,g}$, 704 $HK_{500\,g}$, and 767 $HV_{100\,g}$.

Keywords: Sintering; Grain size; Nanocomposites; Optical properties; Hardness; Y_2O_3

1. Introduction

Transparent poly-crystalline ceramics have found increased interest over the last few years.[1–15] This interest is fueled by potential applications such as windows and domes,[16–18] transparent armor,[19] light bulb envelopes,[20] scintillators,[21] and solid-state laser materials.[22–32] Advantages of poly-crystalline ceramics over single crystals include that they can be formed into a variety of shapes, can usually be produced in larger sizes more cheaply, and have enhanced mechanical and thermo-mechanical properties.

Our research focuses on transparent ceramics for applications as infrared windows. This application requires that the material is mechanically strong, optically transparent over a wide range of wavelengths, and has a low optical emissivity at elevated temperatures. A review of available infrared window materials concluded that the most durable materials, sapphire (Al_2O_3), AlON ($9Al_2O_3{\cdot}5AlN$), and Spinel ($MgAl_2O_4$), all emit too much light at elevated temperatures, and that without the availability of completely new materials, existing materials will have to be engineered by possibly using nanophase starting materials, to meet the optical and mechanical requirements.[18] Decreasing the grain size of a ceramic increases the mechanical strength and thus the resistance to thermal shock—an important consideration for applications such as missile domes and lasers.

One of the materials of interest for transparent windows and domes is poly-crystalline yttria (Y_2O_3).[1,33,34] This material has a much lower emissivity at high temperatures than sapphire, Spinel, and AlON.[16] However, its mechanical properties such as hardness are worse than those of sapphire, Spinel, and AlON. The hardness of a ceramic is inversely proportional to the square root of the grain size.[16] As such, it is expected that the hardness of Y_2O_3 could be enhanced by reducing the grain size.

A reduction in grain size of Y_2O_3 was accomplished by codoping with La_2O_3.[16] However, this codoping negatively affected the specific heat capacity and thus the resistance to thermal shock of this material. The other option to keep the grain size small is to start with nanophase starting material and to limit the overall grain growth. Several researchers have reported on the sinterability of nanophase yttria. Willingham et al. confirmed the superior sinterability of nanophase yttria as compared to conventional yttria powder.[17] Chen and Wang reported on a two-stage sintering process of nanocrystalline ceramics without final-stage grain growth.[35] Merkert et al. reported on grain coarsening and high porosity due to agglomerates in the nanophase starting powder.[36]

As early as 1969, Dutta and Gazza reported on the fabrication of transparent yttria ceramics.[37] These authors used

* Tel.: +1 509 358 7681; fax: +1 509 358 7627.
E-mail address: eilers@wsu.edu.

0955-2219/$ – see front matter © 2007 Elsevier Ltd. All rights reserved.
doi:10.1016/j.jeurceramsoc.2007.04.006

commercially available yttria powder and vacuum hot-pressing to prepare ceramics with an average grain size of 0.5–1 μm, a relative density of above 99.6%, an IR transmittance above 80% (for wavelengths longer than 2 μm), and a Knoop hardness of 900 with a load of 100 g. No transmittance data below 2 μm is given. According to these authors, the most important processing parameters are: temperature at which the initial pressure is applied, the heating rate, and the use of non-reactive spacer materials.

Saito et al. have reported on the fabrication of transparent yttria ceramics at low temperature using carbonate-derived yttria powder.[1] These authors used vacuum sintering and were able to reach almost full density at temperatures as low as 1500 °C. Samples sintered at 1600 °C and 1700 °C reached transmittance values of about 20% and 25–30% at 500 nm, respectively.

Ikegami et al., reported on the fabrication of transparent yttria ceramics using yttrium hydroxide.[38] Doping with sulfate ions and calcination at temperatures above 1000 °C resulted in monodispersed particles which led to transparent ceramics when vacuum sintered at 1700 °C for 1 h.

Recently, Mouzon and Odén reported on the fabrication of transparent Yb:Y_2O_3 ceramics.[39] These authors prepared their own yttria starting material and then used vacuum sintering followed by hot-isostatic pressing (HIP). Depending on how the authors prepared their starting material, they were able to measure transmittances of up to 45% at 500 nm. However, no transmittance data above 850 nm are presented. The authors point out that silicon and aluminum impurities most likely reacted with yttria, forming a liquid phase which influenced the final sintering stages.

We are particularly interested in yttria ceramics with small grain sizes, because of their expected increased mechanical strength and resistance to thermal shock.[16] In order to keep the grain size as small as possible, we chose nanophase starting materials. Our goal was to determine the most promising parameters for a simple and cost-effective fabrication method for yttria ceramics, and we report here on the investigated powder processing, sintering, and characterization of these ceramics.

2. Experimental procedures

2.1. Fabrication of ceramics

Commercially available nanophase yttria powder was purchased from Inframat Advanced Materials, Farmington, CT. The material is 99.95% pure Y_2O_3 (product #39N-0802) with a manufacturer-determined particle size of 30–50 nm (from BET and TEM) and a BET multi-point specific surface area of 30–50 m^2/g. Table 1 lists the impurities from the manufacturer's Certificate of Analysis. The main, non-rare-earth impurities are Si, Ca, and Fe. No additional additives or dopants were added to the yttria powder so as not to negatively affected the specific heat capacity and thus the resistance to thermal shock of this material.[16]

To break up any potential agglomerates in the starting powder, some powder samples were ball-milled using zirconia pellets. Some samples were ball-milled dry, while others were ball-milled wet using deionized water. Typically, about 10 g of yttria were mixed with 200 ml of water and the zirconia pellets took up about 20% of the volume for the wet balling. After the ball-milling was complete, the pellets were removed and the slurry was dried for several hours, either on a hot-plate or in a furnace at temperatures between 80 °C and 150 °C. No measurements of the residual humidity were performed.

Table 1
Impurities in commercial nanophase yttria powder (from Certificate of Analysis, Inframat Advanced Materials, Farmington, CT)

Element	Maximum impurities (ppm)
CaO	50
CuO	10
Fe_2O_3	30
NiO	10
PbO	10
SiO_2	100
ZnO	10
CeO_2	20
Dy_2O_3	20
Er_2O_3	20
Gd_2O_3	20
Ho_2O_3	20
La_2O_3	20
Nd_2O_3	20
Pr_2O_3	20
Sm_2O_3	20
Tb_2O_3	20
Yb_2O_3	20

Green bodies were pressed from as-received and wet (Y_2O_3 and deionized H_2O in a ratio of 2:1) powders using a uniaxial press and stainless steel dies. After drying, the powders were uniaxially pressed into pellets using pressures ranging from 44 MPa to 3.37 GPa, with most samples pressed at about 200 MPa for 15 min. The green bodies were round disks with either 25.4 mm diameter and 3–4 mm thickness, or 12.7 mm diameter and 1–2 mm thickness. No binders were used in the preparation of the ceramics. Typically, wet green bodies were dried in a furnace for 48 h at 150 °C before further processing.

Sintering was performed in a Lindberg/Blue box furnace. Samples were placed inside alumina (99.8% purity) crucibles with lids and placed inside the furnace. For most of the ceramics, the green body was covered in yttria powder during sintering. Samples were either single-stage or two-stage sintered in air. In the single-stage sintering process, the sample was heated in air from room temperature to the desired sintering temperature. The sample soaked for the desired period of time before cooling to room temperature. In the two-stage sintering process, the sample was heated in air from room temperature to an initial peak sintering temperature. The temperature was then immediately reduced to a lower sintering temperature and the sample soaked for the desired period of time. Subsequently, the sample was cooled to room temperature. Unless otherwise noted, typical heating and cooling rates range from 100 °C/h to 400 °C/h. Some samples were subsequently hot-isostatically pressed (HIPped) by Raytheon Corp. HIPping of the ceramics was typically per-

formed at 1650 °C in an Ar pressure of 203 MPa for 6 h. Only samples that had at least a relative density of 98% were hipped.

2.2. Evaluation

Density measurements were performed using Archimedes principle. Throughout this paper we use relative densities, defined as the ratio of actual measured density to theoretical density (the theoretical density for Y_2O_3 is 5.01 g/cm^3). An analysis of the density measurements from nine identically prepared samples yielded a standard deviation of 1.3% for the relative density measurements. For the green-body densities we also used the geometric density and compared the results with the Archimedes density. This comparison provides us with information of the amount of closed porosity in the green bodies.

X-ray diffraction (XRD) was performed on the powder using a Siemens D-500 X-ray powder diffractometer. Powder particles were dispersed in alcohol and then ultrasonicated. The dispersion was then dropped onto a quartz zero background plate and the alcohol allowed to evaporate.

Promising samples were lapped and polished and their optical transmittance measured using a Varian Cary 50 UV–vis spectrophotometer. Some ceramics were etched in 20% aqueous HCl for 3 min to expose grain boundaries and coated with a thin gold layer. Scanning electron microscopy (SEM) was performed using an electron microscope (Hitachi S-570) to investigate the microstructure. Grain sizes were determined from SEM images using the linear intercept method. The apparent grain size was multiplied by 1.56 to yield the actual grain size.[7,40] Hardness measurements were performed using a micro-indenter (LECO LM247AT).

3. Results and discussion

Fig. 1 shows the X-ray diffraction data for the commercial nanophase yttria powder, indicating good crystallinity and confirming the cubic phase of the yttria material. The cubic phase of the yttria powder is required for further successful processing, as

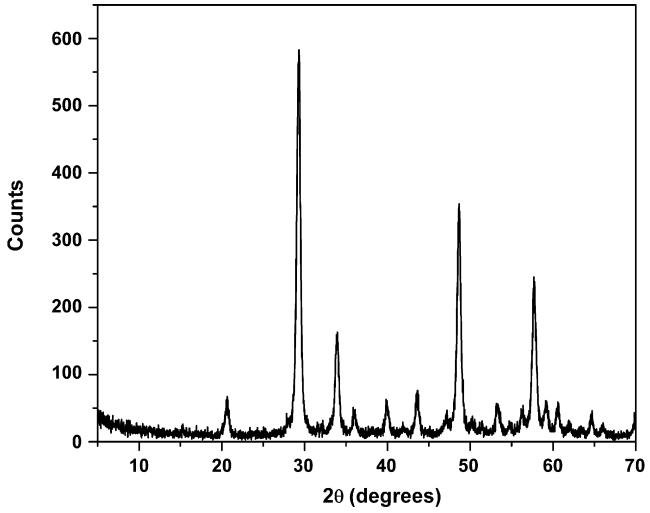

Fig. 1. X-ray diffraction scan of commercial nanophase yttria powder.

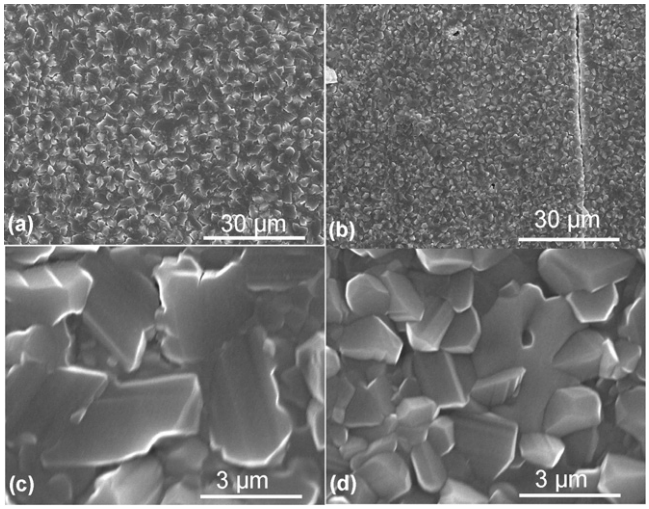

Fig. 2. SEM images of ceramics made from powder A. The sample on the left was fabricated from as-is nanopowder, while the sample on the right was fabricated from ball-milled nanopowder.

the sintering of green bodies made from monoclinic yttria powder leads to the destruction of the samples during sintering.[41] To investigate the potential presence of agglomerates in the commercial yttria powder, we compared ceramics made from ball-milled powder with ceramics made from non-ball-milled (as-received) powder.

Fig. 2 shows a montage of SEM images, comparing these two ceramics. Fig. 2(a) shows a sample prepared from as-received nanophase yttria powder, and Fig. 2(b) shows a sample prepared from ball-milled (4 h) nanophase yttria powder. Fig. 2(c) and (d) show magnified images of these two samples. Both samples were heated to 1500 °C within 1 h, soaked for 12 h and then allowed to cool to room temperature before they were heated up to 1600 °C within 1 h, soaked for 12 h, and then allowed to cool again to room temperature.

Relative densities of these two samples were measured to be 98.5% (as-received nanopowder) and 98.2% (ball-milled nanopowder), indicating that ball-milling does not result in any significant density improvements. Nevertheless, the ceramic prepared from the ball-milled powder appears to have a finer grain structure, compare Fig. 2(c) and (d). Facetted and roughly equiaxed grains are clearly visible in both samples. It appears that ball-milling reduces the size of the particles, which in turn keeps the final grain size of the sintered ceramics smaller. However, the almost identical relative densities of the as-received and the ball-milled samples leads us to conclude that either no significant amount of agglomerates is present in the as-received material, or that ball-milling is not able to break up existing agglomerates.

Next, we investigated the compressibility of the nanophase yttria powder by measuring the density of wet-pressed green bodies. The green bodies were prepared by mixing yttria nanopowder with water, drying the powder, and pressing it into pellets. The sample densities were determined by geometric measurements (weight/volume) and by the Archimedes method and are listed in Table 2. The geometric results are obviously

Table 2
Green-body densities

Sample	Pressure (MPa)	Geometric density	Archimedes
1	211	56.2%	87.6%
2	175	55.6%	88.1%
3	140	54.3%	88.0%
4	105	52.5%	88.1%
5	70	50.0%	88.0%

smaller since the samples contain a certain amount of open porosity and this technique includes these voids in its results. The measurement also reflects the increasing density with increasing pressure. The Archimedes method, which does not average over the open voids, shows a relatively high, but constant density of about 88%. Closed pores cannot fill with water, resulting in the 88% relative density. These densities are comparable to what Kaygorodov et al. reported for green bodies prepared from unagglomerated monoclinic yttria powder.[41] Fig. 3 shows the SEM image of a green body. The relative density of this sample was measured to be about 80% (measured by Archimedes). The Archimedes data in Table 2 do not change with pressure, indicating that the green bodies have a certain fixed amount of closed porosity which is most likely due to agglomerates in the starting powder.[42]

Various sintering protocols for the preparation of transparent ceramics have been reported in the literature.[1,17,35–39] We sintered yttria green bodies at various temperatures and soaking times. Fig. 4 shows a summary of the relative densities of ceramics sintered at various temperatures and soaking times. No dependence of the density on these specific sintering conditions is apparent, indicating again the potential presence of agglomerate-induced pores.[42] Fig. 5 shows two SEM images of air-sintered ceramics. The sample on the left was sintered at 1600 °C for 8 h, while the sample on the right was two-stage sintered (ramped to 1700 °C for 1 min and then soaked for 2 h at 1600 °C). Both of the samples show similar grain sizes and densities, 99.8% and 98.5%, respectively.

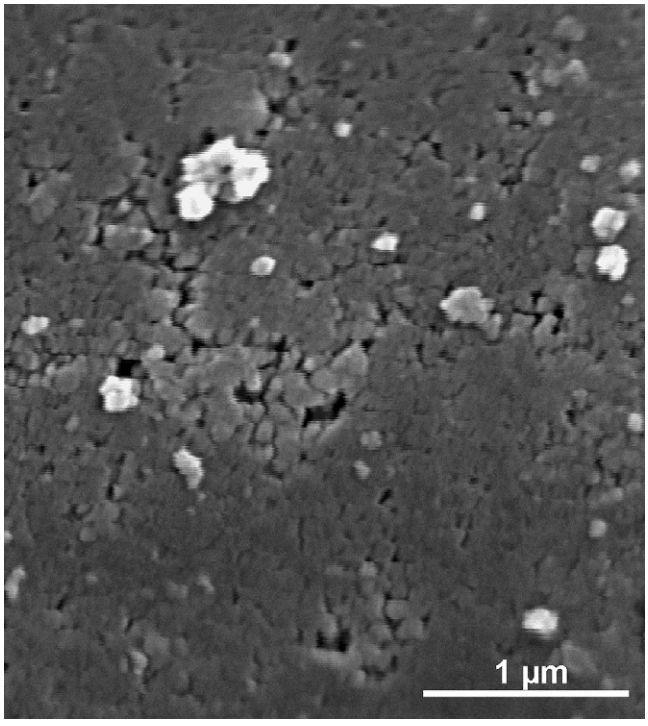

Fig. 3. SEM image of a green body, prepared from a mixture of yttria nanoparticles and water. This sample has a relative density of about 80%.

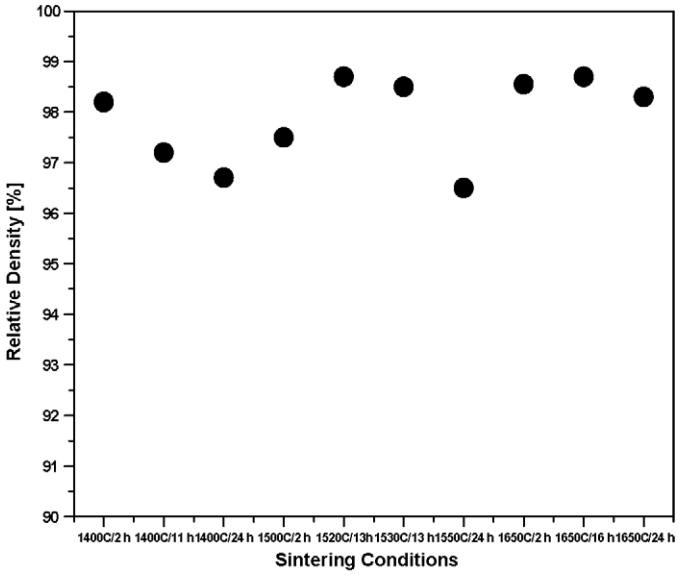

Fig. 4. Relative densities of ceramics, made from powder A for various sintering temperatures and soaking times. All of these samples were single-stage sintered.

To fabricate IR-transparent ceramics we used hot-isostatic pressing (HIP) to take the ceramics to a state of full density and IR-transparency. Nanophase yttria powder was dry-pressed in a stainless steel die under 632 MPa for 30 min, resulting in a 12.7 mm diameter and about 2 mm thick green body. The green body was subsequently sintered at 1600 °C for 2 h in air in a Lindberg/Blue box furnace, resulting in a translucent ceramic with a relative density of about 99.4%. Fig. 6(a) shows an image of the yttria ceramic after lapping and polishing. The unpolished ceramic was about 11 mm in diameter, 1.5 mm thick, and translucent enough to distinguish letters. After lapping and polishing the thickness decreased to about 0.5 mm. The sample flatness was tested with λ/20 optical flats and showed flatness within one to three fringes, with only slight rounding near the outer edge of each face. While letters are visible through the ceramic, the transmittance in the visible wavelength range is limited and we did not take photos with a spacing between the ceramic and background. Apetz and van Bruggen explain the significance of such a spacing in more detail.[20]

Fig. 6(b) shows the transmittance of the 0.5 mm thick polished ceramic yttria sample. Yttria has a theoretical transmittance of just over 80% over the visible and infrared wavelength range. Transmittance spectra of single-crystal yttria and polycrystalline yttria can be found elsewhere.[16] Optical scattering, particularly in the visible wavelength range, limits the transparency of most ceramics.[1,34]

Fig. 7 shows an SEM image of a transparent ceramic after it was etched to expose grain boundaries. Linear intercept and

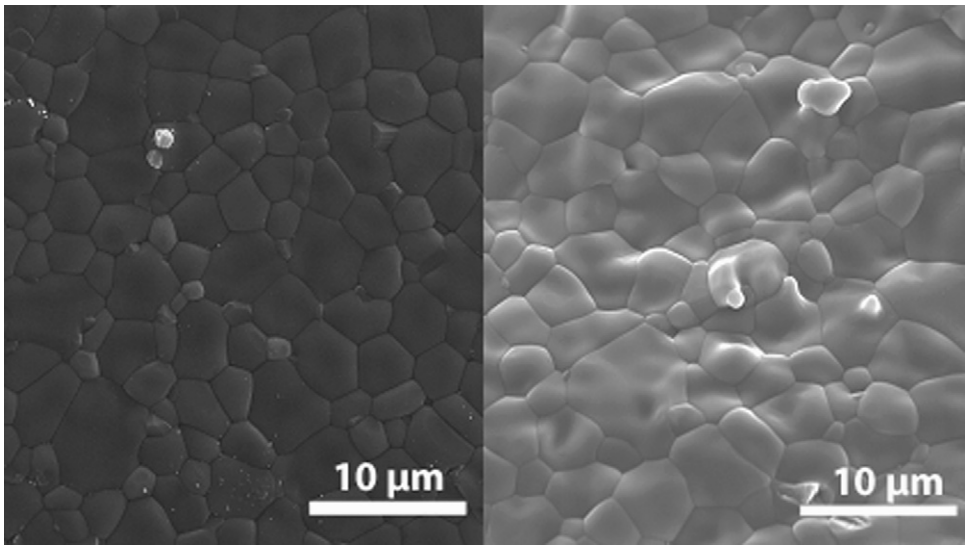

Fig. 5. SEM images of air-sintered yttria ceramics. The sample on the left was sintered for 8 h at 1600 °C, while the sample on the right was ramped to 1700 °C and then soaked for 2 h at 1600 °C.

multiplication with a factor of 1.56 yielded an average grain size of 21.5 ± 11.1 μm. Large pores are visible, further indicating that the less than ideal transparency is due to optical scattering.

The measured grain size of 21.5 μm is significantly larger than the grain size reported by Dutta and Gazza.[37] These authors also reported the use of commercially available nanophase yttria powder and did not use any additional additives. However, they used vacuum hot-pressing at temperatures in the 1300–1500 °C range which is several hundred degrees lower than our sintering and HIPping temperature.

Knoop hardness and Vickers hardness measurements were performed on the polished and etched sample. Measurements showed hardnesses of 792 $HK_{100\,g}$, 704 $HK_{500\,g}$, and 767 $HV_{100\,g}$, in good agreement with published data.[16]

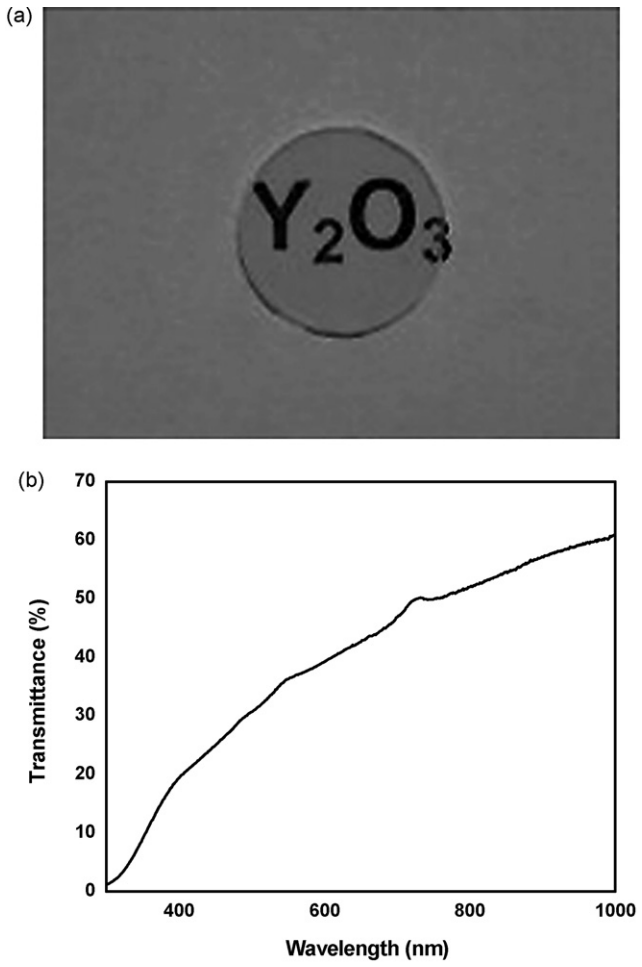

Fig. 6. Image of yttria ceramic after it was lapped and polished (a). Transmittance of polished ceramic yttria sample (b).

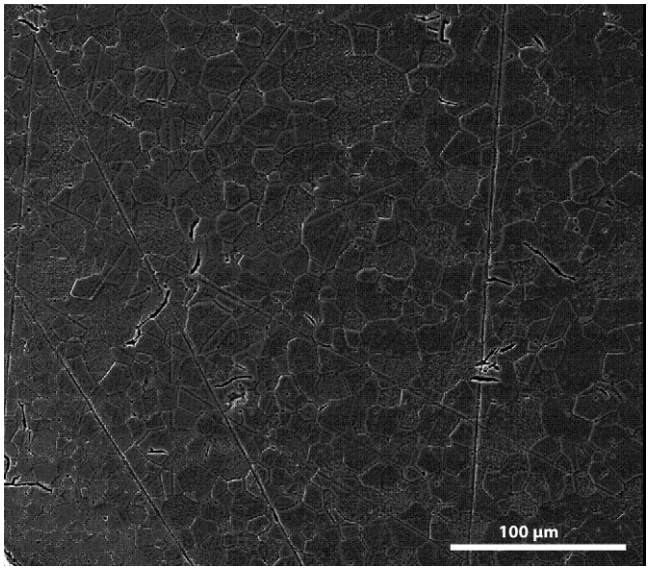

Fig. 7. SEM image of transparent yttria sample. The straight lines were caused by the polishing process.

4. Conclusion

While earlier reports on transparent yttria ceramics have focused on using vacuum sintering in combination with HIPping, our results show that sintering in air in combination with HIPping can also be used to prepare transparent yttria ceramics. Commercially available nanophase yttria powder can easily be processed into green bodies with high densities. The density of the resulting air-sintered ceramics varies very little for processing conditions between 2 h at 1400 °C and 24 h at 1650 °C, indicating that sintering in air limits densities to about 98–99%. HIPping is required to take the ceramics to full density. While the demonstration of IR-transparent ceramics was achieved, the grain size of the ceramics is larger than was hoped. We will further explore the processing conditions of nanophase yttria starting powders with the goal to reduce the ceramic grain size.

Acknowledgements

This work was supported by ONR Grant N00014-03-1-0247. I thank Josh Misner and Fred Hidden for preparing and sintering the ceramics, Nathan Arganbright for lapping, polishing, and hardness measurements, Todd Stefanik at Raytheon for performing the hot-isostatic pressing and for helpful comments, Zbigniew Dreger and Neil Holmes for the transmission measurements, Dan Skorski (supported by the National Science Foundation – 0453554 – through the REU site program at Washington State University), M. Grant Norton, and C. Davitt for help with the SEM measurements, and Dan Harris for helpful comments on the requirements of yttria ceramics.

References

1. Saito, N., Matsuda, S. and Ikegami, T., Fabrication of transparent yttria ceramics at low temperature using carbonate derived powder. *J. Am. Ceram. Soc.*, 1998, **81**, 2023–2028.
2. Tekeli, S. and Gürü, M., The factors affecting colloidal processing of 8YSCZ ceramics. *Key Eng. Mater.*, 2005, **280–283**, 729–734.
3. Macedo, Z. S. and Hernandes, A. C., Laser sintering of bismuth germanate ($Bi_4Ge_3O_{12}$) ceramics. *J. Am. Ceram. Soc.*, 2002, **85**, 1870–1872.
4. Krell, A. and Ma, H. W., Sintering transparent and other sub-μm alumina: the right powder. *cfi-Ceram. Forum Int.*, 2003, **80**(4), E41–E45.
5. Krell, A., Blank, P., Ma, H. and Hutzler, T., Transparent sintered corundum with high hardness and strength. *J. Am. Ceram. Soc.*, 2003, **86**, 12–18.
6. Li, J.-G., Ikegami, T. and Mori, T., Fabrication of transparent, sintered Sc_2O_3 ceramics. *J. Am. Ceram. Soc.*, 2005, **88**, 817–821.
7. Chen, P.-L. and Chen, I.-W., Sintering of fine oxide powders. I. Microstructural evolution. *J. Am. Ceram. Soc.*, 1996, **79**, 3129–3141.
8. Chen, P.-L. and Chen, I.-W., Sintering of fine oxide powders. II. Sintering mechanisms. *J. Am. Ceram. Soc.*, 1997, **80**, 637–645.
9. Lance, D., Valdivieso, F. and Goeuriot, P., Correlation between densification rate and microstructural evolution for pure alpha alumina. *J. Eur. Ceram. Soc.*, 2004, **24**, 2749–2761.
10. Lim, L. C., Wong, P. M. and Ma, J., Colloidal processing of sub-micron alumina powder compacts. *J. Mater. Process. Technol.*, 1997, **67**, 137–142.
11. Lim, L. C., Wong, P. M. and Ma, J., Microstructural evolution during sintering of near-monosized agglomerate-free submicron alumina powder compacts. *Acta Mater.*, 2000, **48**, 2263–2275.
12. Ma, J. and Lim, L. C., Effect of particle size distribution on sintering of agglomerate-free submicron alumina powder compacts. *J. Eur. Ceram. Soc.*, 2002, **22**, 2197–2208.
13. Oliveira, M. I. L. L., Chen, K. and Ferreira, J. M. F., Influence of powder pre-treatments on dispersion ability of aqueous silicon nitride-based suspensions. *J. Eur. Ceram. Soc.*, 2001, **21**, 2413–2421.
14. Oliveira, M. I. L. L., Chen, K. and Ferreira, J. M. F., Influence of the deagglomeration procedure on aqueous dispersion, slip casting and sintering of Si_3N_4-based ceramics. *J. Eur. Ceram. Soc.*, 2001, **22**, 1601–1607.
15. Saito, N., Haneda, H., Sakaguchi, I. and Ikegami, T., Effect of the calcium dopant on oxide ion diffusion in yttria ceramics. *J. Mater. Res.*, 2001, **16**, 2362.
16. Harris, D. C., *Materials for Infrared Windows and Domes*. SPIE Press, Bellingham, WA, 1999.
17. Willingham, C. B., Wahl, J. M., Hogan, P. K., Kupferberg, L. C., Wong, T. Y. and De, A. M., Densification of nano-yttria powders for IR window applications. In *Windows and Dome Technologies VIII, Proceedings of SPIE, vol. 5078*, ed. R. W. Tustison. SPIE, Bellingham, WA, 2003, pp. 179–188.
18. Harris, D. C., Durable 3–5 μm transmitting infrared window materials. *Infrared Phys. Technol.*, 1998, **39**, 185–201.
19. Sands, J. M., Patel, P. J., Dehmer, P. G., Hsieh, A. J. and Boyce, M. C., Protecting the future force: transparent materials safeguard the Army's Vision. *AMPTIAC Quart.*, 2004, **8**, 28–36.
20. Apetz, R. and van Bruggen, M. P. B., Transparent alumina: a light-scattering model. *J. Am. Ceram. Soc.*, 2003, **86**, 480–486.
21. Greskovich, C. and Duclos, S., Ceramic scintillators. *Annu. Rev. Mater. Sci.*, 1997, **27**, 69–88.
22. Lu, J., Song, J., Prabhu, M., Xu, J., Ueda, K., Yagi, H. *et al.*, High-power Nd:$Y_3Al_5O_{12}$ ceramic laser. *Jpn. J. Appl. Phys.*, 2000, **39**, L1048–L1050.
23. Kong, J., Tang, D. Y., Lu, J., Ueda, K., Yagi, H. and Yanagitani, T., Diode-end-pumped 4,2-W continuous-wave Yb:Y_2O_3 ceramic laser. *Opt. Lett.*, 2004, **29**, 1212–1214.
24. Kong, J., Tang, D. Y., Lu, J. and Ueda, K., Spectral characteristics of a Yb-doped Y_2O_3 ceramic laser. *Appl. Phys. B*, 2004, **79**, 449–455.
25. Lupei, V., Lupei, A. and Ikesue, A., Transparent Nd and (Nd,Yb)-doped Sc_2O_3 ceramics as poptential new laser materials. *Appl. Phys. Lett.*, 2005, **86**, 111118.
26. Huie, J. and Gentilman, R., Characterization of transparent polycrystalline yttrium aluminum garnet (YAG) fabricated from nano-powder. In *Windows and Dome Technologies and Materials IX, Proceedings of SPIE, vol. 5786*, ed. R. W. Tustison. SPIE, Bellingham, WA, 2005, pp. 251–257.
27. Eilers, H., Eye-safe Er,Yb:Y_2O_3 ceramic laser materials. In *Windows and Dome Technologies and Materials IX, Proceedings of SPIE, vol. 5786*, ed. R. W. Tustison. SPIE, Bellingham, WA, 2005, pp. 242–250.
28. Li, J.-G., Ikegami, T., Lee, J.-H. and Mori, T., Low-temperature fabrication of transparent yttrium aluminum garnet (YAG) ceramics without additives. *J. Am. Ceram. Soc.*, 2000, **83**, 961–963.
29. Shirakawa, A., Takaichi, K., Yagi, H., Bisson, J.-F., Lu, J., Musha, M. *et al.*, Diode-pumped mode-locked Yb^{3+}:Y_2O_3 ceramic laser. *Opt. Expr.*, 2003, **11**, 2911–2916.
30. Lu, J., Lu, J., Murai, T., Takaichi, K., Uematsu, T., Ueda, K. *et al.*, Nd^{3+}:Y_2O_3 ceramic laser. *Jpn. J. Appl. Phys.*, 2001, **40**, L1277–L1279.
31. Lu, J., Takaichi, K., Uematsu, T., Shirakawa, A., Musha, M., Ueda, K. *et al.*, Promising ceramic laser material: highly transparent Nd^{3+}:Lu_2O_3 ceramic. *Appl. Phys. Lett.*, 2002, **81**, 4324–4326.
32. Lu, J., Bisson, J. F., Takaichi, K., Uematsu, T., Shirakawa, A., Musha, M. *et al.*, Yb^{3+}:Sc_2O_3 ceramic laser. *Appl. Phys. Lett.*, 2003, **83**, 1101–1103.
33. Huang, Z., Sun, X., Xiu, Z., Chen, S. and Tsai, C.-T., Precipitation synthesis and sintering of yttria nanopowders. *Mater. Lett.*, 2004, **58**, 2137–2142.
34. Wen, L., Sun, X., Lu, Q., Xu, G. and Hu, X., Synthesis of yttria nanopowders for transparent yttria ceramics. *Opt. Mater.*, 2006, **29**, 239–245.
35. Chen, I. W. and Wang, X. H., Sintering dense nanocrystalline ceramics without final-stage grain growth. *Nature*, 2000, **404**, 168.
36. Merkert, P., Hahn, H. and Rödel, J., Sintering behaviour of nanocrystalline Y_2O_3. *Nanostruct. Mater.*, 1999, **12**, 701–704.
37. Dutta, S. K. and Gazza, G. E., Transparent Y_2O_3 by hot-pressing. *Mater. Res. Bull.*, 1969, **4**(11), 791–796.
38. Ikegami, T., Li, J.-G., Mori, T. and Moriyoshi, Y., Fabrication of transparet yttria ceramics by the low-temperature synthesis of yttrium hydroxide. *J. Am. Ceram. Soc.*, 2002, **85**, 1725.

39. Mouzon, J. and Odén, M., *Fabrication of transparent yttria by combination of Hot Isostatic Pressing and liquid phase sintering. In Synthesis of Yb:Y_2O_3 nanoparticles and fabrication of transparent polycrystalline yttria ceramics*. Licentiate thesis, Luleå University of Technology, ISSN: 1402-1757, 2005, pp. 107–126.
40. Reed, J. S., *Principles of Ceramic Processing* (*2nd ed.*). Wiley-Intersciences, New York, 1995.
41. Kaygorodov, A. S., Ivanov, V. V., Khrustov, V. R., Kotov, Yu. A., Medvedev, A. I., Osipov, V. V. *et al.*, Fabrication of Nd:Y_2O_3 transparent ceramics by pulsed compaction and sintering of weakly agglomerated nanopowders. *J. Eur. Ceram. Soc.*, 2007, **27**, 1165.
42. Krell, A. and Klimke, J., Effects of the homogeneity of particle coordination on solid-state sintering of transparent alumina. *J. Am. Ceram. Soc.*, 2006, **89**, 1985.